Brownian dynamics simulations of flexible polymers with spring–spring repulsions

Satish Kumar[a] and Ronald G. Larson[b]
Department of Chemical Engineering, University of Michigan, 2300 Hayward, 3074 H. H. Dow Building, Ann Arbor, Michigan 48103

(Received 13 December 2000; accepted 2 February 2001)

We develop a method which incorporates spring–spring repulsions into Brownian dynamics simulations of flexible polymers. The distance of closest approach between two springs is computed, and a repulsive force is then applied based on this distance. Repulsive potentials of the exponential and power-law forms are considered. We demonstrate that our method is capable of accounting for excluded-volume effects in start-up of extensional flow. Equilibrium simulations indicate that spring-spring repulsions can be used to prevent the passage of two springs through each other, and thus maintain the topological integrity of polymer molecules. The method developed here is expected to be useful for simulating entanglement phenomena in both single and multichain systems. © *2001 American Institute of Physics.* [DOI: 10.1063/1.1358860]

I. INTRODUCTION

A distinguishing feature of a polymer molecule is its ability to become entangled with either itself or other polymer molecules. These entanglements are responsible for phenomena such as knotting[1] and reptation[2] which contribute to the remarkable behavior of polymeric liquids.[3] In principle, entanglements could be captured in a molecular-level simulation by modeling the polymers in atomistic detail or with ''pearl necklace'' chains having excluded volume to prevent the passage of one polymer segment through another. In practice, this is not feasible if one would like to simulate entanglement behavior in relatively long polymers (~ 1 μm) over time scales on the order of seconds. At these long time scales, entanglement behavior can be important in a variety of practical settings including rheological characterization, polymer processing, and electrophoretic separation of DNA and proteins.[3,4] Successful molecular-level simulations relevant to these examples thus require the use of a more coarse-grained model for the polymers. One such model is the bead–spring system which is commonly used in Brownian dynamics (BD) simulations (Fig. 1). However, a key limitation of current bead–spring models is that entanglement behavior is not accounted for since the springs are free to pass through each other. In this paper, we develop an idea for overcoming this limitation: the incorporation of spring–spring repulsions into BD simulations.

In a bead–spring model, the beads represent points where the polymer feels a viscous drag while the springs allow the polymer to stretch and orient. In addition to a drag force, each bead is subject to a spring force and a Brownian force. Writing a force balance for each bead and neglecting inertia produces a set of stochastic ordinary differential equations which can then be integrated with respect to time,

$$\frac{d\boldsymbol{r}_i}{dt} = (\boldsymbol{\nabla u})^T \cdot \boldsymbol{r}_i + \frac{1}{\zeta}[\boldsymbol{F}_i^{\mathrm{spr}} - \boldsymbol{F}_{i-1}^{\mathrm{spr}}] + \frac{1}{\zeta}\boldsymbol{B}(t), \tag{1}$$

where $\boldsymbol{r}_i$ is the position vector of bead i, $\boldsymbol{u}$ is the velocity field of the solvent, ζ is the bead drag coefficient, $\boldsymbol{F}_i^{\mathrm{spr}}$ is the force exerted by spring i, and $\boldsymbol{B}(t)$ is the Brownian force. The spring force is generally a nonlinear function of the spring extension.[5] The Brownian force satisfies the fluctuation-dissipation theorem and represents the agitation of the solvent, which is modeled as a thermal bath.[6] [Hydrodynamic interactions between the beads are not included in Eq. (1) but can readily be incorporated.[7,8]] Averaging of the results over time or an ensemble is used to obtain final information about polymer conformations. By choosing the properties of the beads and springs correctly, the rheological behavior of polymers can be accurately simulated.[9–12]

In Eq. (1) there are no forces which prevent two springs from passing through each other, and this can lead to violations of the topological integrity possessed by polymer molecules. One way to prevent spring crossings is to make the maximum spring lengths very short while introducing bead–bead repulsive forces (''pearl necklace'' model).[13,14] However, the short spring lengths preclude efficient long-time simulation of large polymers (e.g., DNA) having contour lengths on the order of microns. A similar issue arises if one uses a bead–rod model since the rod lengths are very short (~ 1 Kuhn length). An alternative method for preventing spring crossings is to incorporate spring–spring repulsions into BD simulations, which is the idea explored in the present manuscript.

We discuss the way in which we account for spring–spring repulsions in Sec. II. In Sec. III, we use the case of start-up of extensional flow to demonstrate that putting spring–spring repulsions into BD simulations can account for excluded-volume effects. In Sec. IV, we develop and

[a]Present address: Department of Chemical Engineering and Materials Science, University of Minnesota, 151 Amundson Hall, 421 Washington Ave. SE, Minneapolis, Minnesota 55455.
[b]Phone: (734) 936-0772; Fax: (734) 763-0459; electronic mail: rlarson@engin.umich.edu

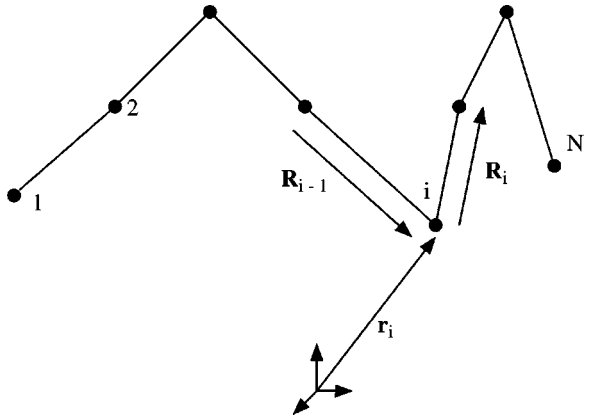

FIG. 1. Bead–spring model of a polymer molecule. Each chain has N beads and $N-1$ springs. The $\boldsymbol{r}_i$ are the position vectors of the beads while the $\boldsymbol{R}_i$ characterize the directions and lengths (magnitudes) of the springs.

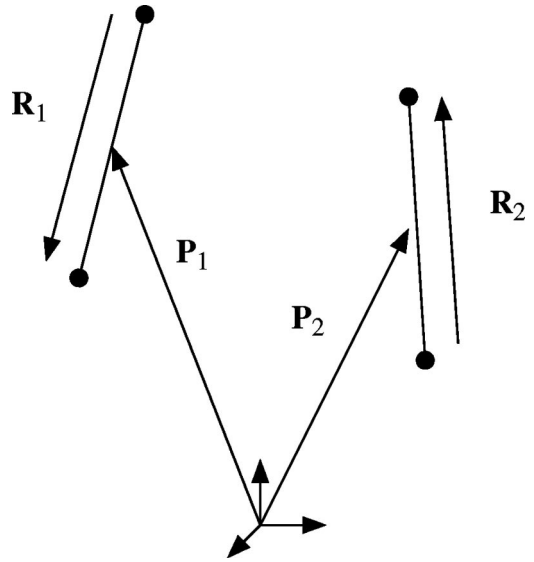

FIG. 2. Vectors used in modeling spring–spring interactions. The $\boldsymbol{R}_i$ characterize the directions and lengths (magnitudes) of the springs while the $\boldsymbol{P}_i$ are the position vectors of the spring midpoints.

verify a method for detecting violations of topological integrity in BD simulations. Finally, our conclusions are presented in Sec. V.

II. SPRING–SPRING REPULSIONS

The general way in which we account for spring–spring repulsions involves computing the distance of closest approach between two springs and imposing a repulsive force based on that distance. Consider two springs, referred to as 1 and 2, which have midpoints $\boldsymbol{P}_1$ and $\boldsymbol{P}_2$. Let $\boldsymbol{R}_1$ and $\boldsymbol{R}_2$ be the vectors characterizing the direction and length (magnitude) of each spring (Fig. 2). Each spring lies on a line, and the distance vector between these lines, $\boldsymbol{D}$, is given by

$$\boldsymbol{D}=\boldsymbol{P}_1+t_1\boldsymbol{R}_1-(\boldsymbol{P}_2+t_2\boldsymbol{R}_2), \tag{2}$$

where t_1 and t_2 are parameters which indicate where we are along each line. The distance of closest approach between the lines is found by minimizing the magnitude of $\boldsymbol{D}$ with respect to t_1 and t_2. This requires that

$$\frac{\partial D^2}{\partial t_1}=\frac{\partial D^2}{\partial t_2}=0, \tag{3}$$

where $D^2=\boldsymbol{D}\cdot\boldsymbol{D}$. Solving Eq. (3) produces the following expressions for t_1 and t_2:

$$t_1=\frac{(\boldsymbol{P}_1-\boldsymbol{P}_2)\cdot(R_2^2\boldsymbol{R}_1-R_{21}\boldsymbol{R}_2)}{R_{21}^2-R_1^2R_2^2}, \tag{4}$$

$$t_2=\frac{(\boldsymbol{P}_2-\boldsymbol{P}_1)\cdot[R_1^2\boldsymbol{R}_2-R_{21}\boldsymbol{R}_1]}{R_{21}^2-R_1^2R_2^2}, \tag{5}$$

where $R_1^2=\boldsymbol{R}_1\cdot\boldsymbol{R}_1$, $R_2^2=\boldsymbol{R}_2\cdot\boldsymbol{R}_2$, and $R_{12}=\boldsymbol{R}_1\cdot\boldsymbol{R}_2$.

For a spring between beads i and $i+1$, we can take $\boldsymbol{P}_i=(\boldsymbol{r}_i+\boldsymbol{r}_{i+1})/2$ and $\boldsymbol{R}_i=\boldsymbol{r}_{i+1}-\boldsymbol{r}_i$. If $-0.5\leqslant t_i\leqslant 0.5$, then the distance of closest approach lies on the spring. If $t_i>0.5$ or $t_i<-0.5$, we assume that the distance of closest approach should be measured from a spring end. This is enforced by setting $t_i=0.5$ or $t_i=-0.5$, respectively. Once we have the appropriate values of t_1 and t_2, we can compute the corresponding value of D from Eq. (2).

The next step is to impose a repulsive force between two interacting springs. Spring 1 will feel this force in the direction of $\boldsymbol{D}$ while spring 2 will feel it in the opposite direction. Since BD simulations are carried out by integrating force balances on beads, the repulsive spring force must be converted into bead forces. To do this, we use a simple lever-rule relation. For spring i, bead i gets a fraction of the force equal to $0.5-t_i$ while bead $i+1$ gets the remainder. We denote the magnitude of the repulsive force by F^{rep} and assume that it can be derived from a corresponding potential U^{rep}, viz., $F^{\mathrm{rep}}=-\partial U^{\mathrm{rep}}/\partial D$. In this work, we describe U^{rep} with either an exponential function,

$$U^{\mathrm{rep}}=Ae^{-\alpha D}, \tag{6}$$

or a power-law function, which we choose to be the repulsive part of the Lennard-Jones potential,

$$U^{\mathrm{rep}}=4\epsilon\left(\frac{\sigma}{D}\right)^{12}, \tag{7}$$

where A and ϵ are the strengths and α and σ are the ranges for the potentials. Similar potentials have been used in previous BD simulations with bead–bead repulsions.[15–17] Once the magnitudes and directions of all the repulsive forces acting on a given bead are known, they are divided by ζ and added to the right-hand side of Eq. (1). In our simulations, we consider single polymer molecules (i.e., dilute solutions) in which each spring interacts with every other nonadjacent spring. The method developed here could also be applied to multichain systems in order to simulate the dynamics of nondilute solutions.

In order to ensure that topological integrity is maintained, the repulsive force must diverge as the interspring separation vanishes. The force associated with Eq. (7) satisfies this requirement but is computationally expensive to implement since its steepness requires the use of very small time steps.[16,18] This problem becomes particularly acute

when trying to verify that the obtained results converge as the time step gets smaller. Much larger time steps can be taken if Eq. (6) is implemented, but there is no guarantee that spring-spring crossings will be prevented. Recognizing the difficulties associated with Eq. (7), we use Eq. (6) to validate the idea of incorporating spring–spring repulsions into BD simulations. We do this by performing simulations for start-up of extensional flow and showing that our results agree with experimental data and with simulations which use more conventional repulsive bead forces rather than spring forces (Sec. III). We then use Eq. (7) in computationally less expensive equilibrium simulations to show that topological integrity can indeed be maintained by applying spring–spring repulsions (Sec. IV).

III. START-UP OF EXTENSIONAL FLOW

Much effort has been devoted to BD simulations of polymers in extensional flows.[9–13,18–21] These flows are of great interest because they play a central role in polymer processing operations and rheological measurement techniques. In one recent work, Li and Larson used BD simulations to study start-up of uniaxial extensional flow of dilute polystyrene (PS) Boger fluids.[12] A bead–spring model was used to describe the polymer, and bead–bead repulsions were incorporated to study the effects of solvent quality. Here, we perform a similar study but use spring–spring repulsions in place of bead–bead repulsions.

We now discuss in more detail the form of each of the terms in Eq. (1). In our simulations, the spring forces are described by Cohen's Padé approximation to the inverse Langevin function,[22]

$$\boldsymbol{F}_i^{\mathrm{spr}}=\frac{k_BT}{b_K}\lambda_i\frac{3-\lambda_i^2}{1-\lambda_i^2}, \tag{8}$$

where

$$\lambda_i=\frac{|\boldsymbol{r}_{i+1}-\boldsymbol{r}_i|}{N_{K,s}b_k}, \tag{9}$$

$N_{K,s}$ is the number of Kuhn steps per spring, b_K is the Kuhn step length, k_B is Boltzmann's constant, and T is the absolute temperature. For uniaxial extensional flow, the velocity gradient is

$$(\boldsymbol{\nabla u})^T=\begin{pmatrix}\dot{\epsilon} & 0 & 0\\ 0 & -\dot{\epsilon}/2 & 0\\ 0 & 0 & -\dot{\epsilon}/2\end{pmatrix}, \tag{10}$$

where $\dot{\epsilon}$ is the extension rate. The Brownian force term is given by

$$\boldsymbol{B}(t)=\sqrt{\frac{6\zeta k_BT}{\Delta t}}\boldsymbol{n}_i(t), \tag{11}$$

where $\boldsymbol{n}_i(t)$ is a vector in which each component is a random number drawn from a uniform distribution over $[-1,1]$ and Δt is the size of the simulation time step. As in Ref. 12, Eq. (1) is integrated using the forward Euler method.

TABLE I. List of parameters used in the BD simulations for extensional flow. The first four parameters are the same for both solvents. The total number of Kuhn steps in the chain is given by N_K.

$N_K=2626$ $b_K=0.001\,803$ μm $T=298$ K $\Delta t=5\times10^{-7}$ s		
	Theta solvent	Good solvent
ζ/k_BT (s/μm^2)	367.5	3335
ν (molecules/μm^3)	239.8	160.5
η_0 (Pa s)	30.96	87.5
$\dot{\epsilon}$ (s^{-1})	5.05	4.9

The experimental data to which we will compare our simulation results is for polystyrene with a molecular weight of $\sim2\times10^6$ g/mol in both theta and good solvents.[23,24] The theta solvent is a solution of low-molecular-weight PS in dioctyl phthalate and the good solvent is ''piccolastic,'' a low-molecular-weight PS. The parameters used in our simulation are mostly the same as those used by Li and Larson and are listed in Table I.[10,12] To simulate behavior in theta solvents, we leave out all spring–spring repulsions and use a 20-bead chain. To simulate behavior in good solvents, we apply Eq. (6) to describe spring-spring repulsions and also use a 20-bead chain. The parameters in Eq. (6) are chosen so that the equilibrium time-averaged radius-of-gyration matches that of the experiments for PS in a good solvent ($\sim$55%–60% greater than the theta value).[12,25] The appropriate values that accomplish this are $A=7k_BT$ and $\alpha=4/b$, where $b=\sqrt{N_{K,s}b_K^2}$ is the root-mean-square spring length. We note that the potential range, α, is comparable to the root-mean-square spring length, as was the case in simulations using bead–bead repulsions.[16,17] This allows one to take time steps which are relatively large. In both the theta and good solvent cases, we apply ensemble averaging to obtain final results; the ensemble size is 50. Initial conditions are obtained by sampling the results of the code in the absence of flow at intervals approximately equal to one relaxation time.

Figure 3 shows the results of our calculation in the form of a plot of the Trouton ratio vs the Hencky strain. The Hencky strain is simply the product of the extension rate and time while the Trouton ratio is the ratio of the uniaxial extensional viscosity to the zero-shear viscosity, $\overline{\eta_u}/\eta_0$.[26] The uniaxial extensional viscosity is the ratio $(\sigma_{11}-\sigma_{22})/\dot{\epsilon}$, with ''1'' in the stretch direction, where the stress tensor is given by[5]

$$\boldsymbol{\sigma}=\eta_s(\boldsymbol{\nabla u}+(\boldsymbol{\nabla u})^T)+\nu\sum_{i=1}^{N-1}\langle\boldsymbol{F}_i^{\mathrm{spr}}\boldsymbol{R}_i\rangle-\nu(N-1)k_BT\boldsymbol{\delta}. \tag{12}$$

Here, ν is the number of polymer molecules per unit volume, η_s is the solvent viscosity, N is the number of beads, $\boldsymbol{\delta}$ is the unit tensor, and the angle brackets represent an ensemble average. For both solvents, Fig. 3 shows good agreement between our simulations and the experiments. We also see

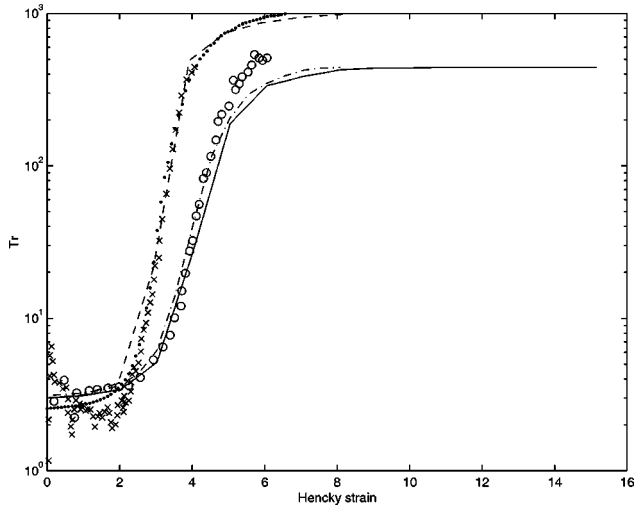

FIG. 3. Trouton ratio vs Hencky strain for start-up of extensional flow. The dashed line represents our simulation results for the good solvent and the crosses are the corresponding experimental values. The dotted line represents the results of a simulation where bead–bead repulsions are used (Ref. 12). The solid line represents our simulation results for the theta solvent and the circles are the corresponding experimental values. The dashed–dotted line represents the results of a simulation where bead–bead repulsions are used (Ref. 12).

that there is good agreement in the good-solvent case between our simulations and those where bead–bead repulsions are used with parameters chosen to obtain a similar equilibrium coil size (i.e., a time-averaged radius-of-gyration 55%–60% greater than the theta value, cf. Fig. 6 of Ref. 12). There is a tendency for our simulations to underpredict the Trouton ratio for the theta solvent at larger Hencky strains, but this is also seen in the simulations that use bead–bead repulsions.[12] The good agreement between our results and both the experimental data and the simulations with bead–bead repulsions indicates that incorporating spring–spring repulsions is a valid alternative to bead–bead repulsions as a means of including excluded-volume effects in BD simulations. In addition, spring–spring repulsions can serve to impose entanglement constraints, as discussed in the next section.

IV. STUDY OF TOPOLOGICAL INTEGRITY

In order to ensure that the topological integrity of polymer molecules is maintained, one must have a way of detecting spring crossings. We do this by determining whether the movement of a given spring intersects any other spring, as illustrated in Fig. 4. After a bead is moved from $\boldsymbol{r}_i(t)$ to $\boldsymbol{r}_i(t+\Delta t)$, we consider two triangular subregions: one formed by $\boldsymbol{r}_i(t)$, $\boldsymbol{r}_i(t+\Delta t)$, and $\boldsymbol{r}_{i+1}(t)$ and the other by $\boldsymbol{r}_i(t)$, $\boldsymbol{r}_i(t+\Delta t)$, and $\boldsymbol{r}_{i-1}(t+\Delta t)$. If a spring not attached to bead i intersects either of these subregions, a spring crossing has occurred.

Following the notation of Sec. II, the line passing through a spring can be described as $\boldsymbol{P}_i+t_i\boldsymbol{R}_i$. The plane containing one of the subregions described above is given by the equation $(\boldsymbol{x}-\boldsymbol{r}_i(t))\cdot\boldsymbol{n}=0$, where $\boldsymbol{n}$ is a normal vector to the subregion. Now, letting $\boldsymbol{x}=\boldsymbol{P}_i+t_i\boldsymbol{R}_i$, we can solve for t_i and obtain the intersection point, $\boldsymbol{x}^*$. If $|t_i|>0.5$, then the spring does not intersect the plane. If $|t_i|\leqslant 0.5$, the spring

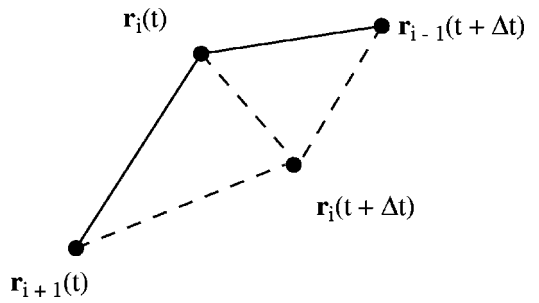

FIG. 4. Triangular subregions used in determining violations of topological integrity. When bead i moves from $\boldsymbol{r}_i(t)$ to $\boldsymbol{r}_i(t+\Delta t)$, we can form two triangular subregions: one with $\boldsymbol{r}_{i+1}(t)$ and the other with $\boldsymbol{r}_{i-1}(t+\Delta t)$. The solid lines represent springs and form one edge of each subregion while the dashed lines denote the other edges.

does intersect the plane and we now have to determine whether or not $\boldsymbol{x}^*$ lies in the subregion. This is easily done by considering the vectors $\boldsymbol{x}^*-\boldsymbol{r}_i(t)$ and $\boldsymbol{x}^*-\boldsymbol{r}_i(t+\Delta t)$ and the angles they form with the vectors which make up the sides of the triangular subregion.

Because almost all of the springs have to be checked after each bead moves, implementing the above procedure is rather time consuming. Thus, here we use it only in equilibrium calculations, which take much less time than the extensional flow calculations. We carried out calculations based on the good solvent PS system discussed in Sec. III. For the repulsive potential based on Eq. (7), we find that $\epsilon=k_BT$ and $\sigma=0.71b$ gives the appropriate radius-of-gyration[27] (i.e., a time-averaged radius-of-gyration 55%–60% greater than the theta value). We note that the potential range, σ, is comparable to that used in Ref. 18, where a Lennard-Jones potential was applied. When we implement a spring-spring repulsive force based on the exponential potential, Eq. (6), we detect a number of topological violations. This is expected since the repulsive force has a finite maximum value which can be overcome if the forces driving two springs toward each other are sufficiently strong. When we use a repulsive force based on the power-law potential, Eq. (7), we detect no topological violations. Thus, incorporating spring-spring repulsions into BD simulations can maintain the topological integrity of polymer molecules if the repulsive force diverges as the interspring distance vanishes. We note that due to the steepness of Eq. (7), the time step required for a stable run is two orders of magnitude smaller than what one can use with Eq. (6).

V. DISCUSSION AND CONCLUSIONS

In this work, we have demonstrated the feasibility of incorporating spring–spring repulsions into BD simulations of flexible polymers. Our simulation results are in good agreement with experimental data on start-up of extensional flow as well as with previous simulations using bead–bead repulsions, and we have shown through equilibrium simulations that our method is capable of maintaining topological integrity if one uses a potential which diverges as the interspring distance vanishes [e.g., Eq. (7)]. We note that the good agreement for extensional flow occurs in spite of the fact that we use an exponential potential, which does not

guarantee that topological integrity is maintained. This is a signal that self-entanglements such as knotting are probably not important in the experiments, and justifies the use of bead–bead repulsions in previous simulations.[12] This may not be true in other experiments where the polymers are longer or less swollen. There, we expect that the probability of self-entanglements will be much higher. More generally, our results imply that if simulations using bead–bead interactions produce results in agreement with analytical or experimental results, then self-entanglement phenomena are probably not important.

The principal limitation of these simulations is the need to take very small time steps when using the power-law potential. We find in some simulations that two springs occasionally get so close together that there is a very large repulsion, resulting in a large increase in the radius-of-gyration. This suggests that smaller time steps are needed so that the springs more gradually feel the repulsive force. We think that one way to overcome this problem in an efficient manner is to use an adaptive time-stepping scheme, and we are currently developing such a code. Large speed-ups may also be obtained by more efficiently accounting for spring–spring repulsions through the use of cell structures and linked lists.[28]

Another challenge for future work is to determine if it is possible to maintain topological integrity without swelling the equilibrium coil size. This might be accomplished by adding an attractive component to the spring–spring repulsions (analogous to what is done in simulations where there are only bead–bead interactions[18]) or by using bead–bead attractions in addition to spring–spring repulsions. Such simulations would be useful for studying polymer entanglements in theta solvents.

In addition to providing a tool for studying self-entanglements of polymers, the method we have developed should prove useful in simulating the behavior of semidilute and concentrated polymer solutions over relatively long time scales. At present, such simulations are unable to reproduce experimental observations because they do not account for entanglements.[29,30] Incorporating spring–spring interactions into BD simulations will also help in the modelling of dilute-solution electrophoresis, where entanglements between a DNA molecule and a polymer molecule help determine separation efficiency.[4] Improved BD simulations of all of these situations would greatly benefit a diverse range of applications including rheological characterization, polymer processing, and genomics.

ACKNOWLEDGMENT

This work was made possible by a grant from the National Science Foundation, CTS-9707778.

[1] R. C. Armstrong, S. K. Gupta, and O. Basaran, Polym. Eng. Sci. **20**, 466 (1980).
[2] M. Doi and S. F. Edwards, *The Theory of Polymer Dynamics* (Oxford University Press, Oxford, 1986).
[3] R. B. Bird, R. C. Armstrong, and O. Hassager, *Dynamics of Polymeric Liquids* (Wiley, New York, 1987), Vol. 1.
[4] M. E. Starkweather, M. Muthukumar, and D. A. Hoagland, Macromolecules **31**, 5495 (1998).
[5] R. B. Bird, C. F. Curtiss, R. C. Armstrong, and O. Hassager, *Dynamics of Polymeric Liquids* (Wiley, New York, 1987), Vol. 2.
[6] W. B. Russel, D. A. Saville, and W. R. Schowalter, *Colloidal Dispersions* (Cambridge University Press, Cambridge, 1989).
[7] D. L. Ermak and J. A. McCammon, J. Chem. Phys. **69**, 1352 (1978).
[8] R. M. Jendrejack, M. D. Graham, and J. J. de Pablo, J. Chem. Phys. **113**, 2894 (2000).
[9] R. G. Larson, H. Hu, D. E. Smith, and S. Chu, J. Rheol. **43**, 267 (1999).
[10] L. Li, G. Larson, and T. Sridhar, J. Rheol. **44**, 291 (2000).
[11] J. S. Hur, E. S. G. Shaqfeh, and R. G. Larson, J. Rheol. **44**, 713 (2000).
[12] L. Li and R. G. Larson, Rheol. Acta **39**, 419 (2000).
[13] S. W. Fetsko and P. T. Cummings, J. Rheol. **39**, 285 (1995).
[14] E. Ben-Naim, G. S. Grest, T. A. Witten, and A. R. C. Baljon, Phys. Rev. E **53**, 1816 (1996).
[15] Z. Xu, S. Kim, and J. J. de Pablo, J. Chem. Phys. **101**, 5293 (1994).
[16] A. Rey, J. J. Freire, and J. García de la Torre, Polymer **33**, 3477 (1992).
[17] K. D. Knudsen, J. García de la Torre, and A. Elgsaeter, Polymer **37**, 1317 (1996).
[18] J. G. Hernández Cifre and J. García de la Torre, J. Rheol. **43**, 339 (1999).
[19] P. S. Doyle, E. S. G. Shaqfeh, and A. P. Gast, J. Fluid Mech. **334**, 251 (1997).
[20] P. S. Doyle and E. S. G. Shaqfeh, J. Non-Newtonian Fluid Mech. **76**, 43 (1998).
[21] P. S. Doyle, E. S. G. Shaqfeh, G. H. McKinley, and S. H. Spiegelberg, J. Non-Newtonian Fluid Mech. **76**, 79 (1998).
[22] A. Cohen, Rheol. Acta **30**, 270 (1991).
[23] N. V. Orr and T. Sridhar, J. Non-Newtonian Fluid Mech. **82**, 203 (1999).
[24] T. Sridhar, D. A. Nguyen, and G. G. Fuller, J. Non-Newtonian Fluid Mech. **90**, 299 (2000).
[25] M. J. Solomon and S. J. Muller, J. Polym. Sci., Part B: Polym. Phys. **34**, 181 (1996).
[26] R. G. Larson, *The Structure and Rheology of Complex Fluids* (Oxford, New York, 1999).
[27] For the power-law potential, we applied a cutoff distance equal to $2^{1/6}\sigma$. To within statistical error, the time-averaged radius-of-gyration remained the same when the time step was decreased by a factor of 2. No cutoff distance was applied for the exponential potential.
[28] M. P. Allen and D. J. Tildesley, *Computer Simulation of Liquids* (Oxford, New York, 1987).
[29] C. Xiao and D. M. Heyes, Phys. Rev. E **60**, 5757 (1999).
[30] C. Xiao and D. M. Heyes, J. Chem. Phys. **111**, 10694 (1999).